

Received June 25, 2020, accepted September 1, 2020, date of publication September 21, 2020, date of current version September 29, 2020.

Digital Object Identifier 10.1109/ACCESS.2020.3025370

A Multiplex Connectivity Map of Valence-Arousal Emotional Model

AVRAAM D. MARIMPI^{1,2,8}, STAVROS I. DIMITRIADIS^{1,2,3,4,5,6,7}, AND RAINER GOEBEL^{1,8}

¹Department of Cognitive Neuroscience, Faculty of Psychology and Neuroscience, Maastricht University, 6229 Maastricht, The Netherlands

²Cardiff University Brain Research Imaging Center (CUBRIC), Neuroinformatics Group, School of Psychology, Cardiff University, Cardiff CF10 3AT, U.K.

³School of Medicine, Institute of Psychological Medicine and Clinical Neurosciences, Cardiff University, Cardiff CF14 4YS, U.K.

⁴Cardiff University Brain Research Imaging Center (CUBRIC), School of Psychology, Cardiff University, Cardiff CF10 3AS, U.K.

⁵School of Psychology, Cardiff University, Cardiff CF10 3AS, U.K.

⁶Neuroscience and Mental Health Research Institute, Cardiff University, Cardiff CF10 3AT, U.K.

⁷MRC Centre for Neuropsychiatric Genetics and Genomics, School of Medicine, Cardiff University, Cardiff CF14 4YS, U.K.

⁸Brain Innovation B.V., 6229 Maastricht, The Netherlands

Corresponding author: Avraam D. Marimpis (avraam.marimpis@maastrichtuniversity.nl)

The work of Avraam D. Marimpis was supported by Brain Innovation B.V., Maastricht, The Netherlands. The work of Stavros I. Dimitriadis was supported in part by an Medical Research Council (MRC) (Behavioural and Neurophysiological Effects of Schizophrenia Risk Genes: A Multi-Locus, Pathway Based Approach) under Grant MR/K004360/1 and in part by a MARIE-CURIE COFUND EU-UK Research Fellowship.

ABSTRACT A high number of studies have already demonstrated an electroencephalography (EEG)-based emotion recognition system with moderate results. Emotions are classified into discrete and dimensional models. We focused on the latter that incorporates valence and arousal dimensions. The mainstream methodology is the extraction of univariate measures derived from EEG activity from various frequencies classifying trials into low/high valence and arousal levels. Here, we evaluated brain connectivity within and between brain frequencies under the multiplexity framework. We analyzed an EEG database called DEAP that contains EEG responses to video stimuli and users' emotional self-assessments. We adopted a dynamic functional connectivity analysis under the notion of our dominant coupling model (DoCM). DoCM detects the dominant coupling mode per pair of EEG sensors, which can be either within frequencies coupling (intra) or between frequencies coupling (cross-frequency). DoCM revealed an integrated dynamic functional connectivity graph (IDFCG) that keeps both the strength and the preferred dominant coupling mode. We aimed to create a connectomic mapping of valence-arousal map via employing features derive from IDFCG. Our results outperformed previous findings succeeding to predict in a high accuracy participants' ratings in valence and arousal dimensions based on a flexibility index of dominant coupling modes.

INDEX TERMS Affective computing, computational neuroscience, emotion in human-computer interaction, graph theory, modeling from video, modeling human emotion, music, neuroscience, video.

I. INTRODUCTION

In the last thirty years of active research, even before the mass commercialization of personal computers, the study of music and how it affects the human brain enjoyed much attention and drew researchers from the different interdisciplinary fields [1]. Emotions play a key role in daily human communication and can be expressed either verbally [2] or via non-verbal cues like gestures, voice, and facial expressions [3]. [4].

The associate editor coordinating the review of this manuscript and approving it for publication was Ting Li ¹.

Emotion detection systems via electroencephalogram (EEG) opens a large variety of important applications for medicine and scientific research [5] and to the field of affective computing [6]. There are multimedia environments designed to recognize human emotional states like recommendation and tagging systems, films, games, and also biofeedback systems based on headsets that might help target groups with, e.g. depression to control their emotional states [7].

Music can induce emotions and impact the mood of individuals [8]. Implicit (generating subjective and emotional tags) tagging of music videos using affective emotional information can benefit a recommendation and retrieval system to

improve its performance [9], and for the design of a personalized music recommendation system [10].

Specifically, users' emotions while watching a music video clip will train a recommender system to recommend successfully a music clip that matches users' current emotional state. Patterns of EEG activity succeeded in discriminating at some level the different valence and arousal levels. For example, asymmetrical patterns of frontal EEG activity have been shown to distinguish between high and low arousal levels [11]. A famous multimodal dataset called DEAP (Database for Emotional Analysis using Physiological Signals) attracted the scientific interest of many research studies to present their results as an attempt to define the best EEG-based descriptors of human emotion induced by music video clips [11].

DEAP database contains the electroencephalographic (EEG) activity and peripheral physiological signals of 32 participants who were recorded while watching 40 one-minute-long excerpts of music videos. Participants rated each video in terms of the levels of arousal, valence, like/dislike, dominance, and familiarity.

The original article presented the DEAP database reported a 62.0 % for low-high arousal and a 57.6% for low-high valence classification. A recent study reported an improvement with 74.3 % for low-high arousal and 77.2% for low-high valence classification tasks [12]. Another study reported the first results from a static connectivity analysis incorporating the richness of spatiotemporal EEG brain activity from 1 min into a single functional brain network. Reported classification results at around 78% [13]. In [14], the authors studied another aspect of the emotion activated patterns, their stability. Working on the DEAP dataset, and another in-house dataset, they proposed that the emotional state is defined in a continuous space and emotional states are dynamically evolving. For that reason, they employed a smoothing technique over their numerous selected features (a linear dynamic system), to filter out components which are not associated with emotional states. In the end, they compare multiple, multiclass classification methods with the maximum reported score of 69.67% accuracy.

Recently, many research studies attempted to adapt brain connectivity as a proper framework to explore the dimensions of emotion and to improve emotion recognition [15]–[17]. Brain connectivity can inform us about how different brain areas communicate [18] and are encapsulating complementary information compared to brain activity [19]. Brain subnetwork over frontal brain areas plays a control role for emotions [20]. Increased delta activity (synchronization) has been reported in both pleasant and unpleasant stimuli [21] while increased delta connectivity has been found after listening to music [22]. Functional phase connectivity in both beta and gamma bands has been associated with auditory and motor functions linked to listening to music [23]. However, most studies so far analyzed EEG recordings across different experimental paradigms focusing solely on within-frequency

coupling, leaving unexplored the notion of cross-frequency coupling.

Several researchers explored the contribution of frontal EEG asymmetry to the understanding of emotional processing [24]. Frontal EEG asymmetry refers to the hemispheric difference of brain activity in various frequencies between EEG sensors located over the left or right frontal area. They reported emotion recognition under this framework [25]. Positive emotions are associated with a left-hemispheric asymmetry of brain activity, while negative emotions with a right-hemispheric activity [26], [27]. Frontal asymmetry has been reported in a brain connectivity context [18]. In other studies, they reported no change in functional asymmetry after an auditory stimulus [28].

In other words, research about the brain mechanisms associated with frontal asymmetry is necessary.

At the same time, a few papers that adopted a brain connectivity analysis restricted their analysis in static brain networks instead of dynamic functional connectivity analysis [13], [29], [31]. Secondly, the emotion recommendation system was designed as two separate two-class binary classification problems instead of a four-class problem or better as a regression analysis that can predict the valence-arousal personal assessment more accurately. Third, the scientific results so far have not provided to the community of affecting computing and emotional BCI systems an accurate emotional recommendation system. Classification results are too low to support a real application scenario [29].

Here, we adopted a dynamic functional connectivity analysis incorporating into an integrated dynamic functional connectivity graph (IDFCG) both the dominant coupling mode and the strength of functional coupling [30]. We searched for dominant coupling mode for each pair of EEG sensors and across temporal segments among within frequencies coupling modes (intra) and between frequencies coupling modes (cross-frequency coupling -CFC). Finally, the IDFCG keeps the type of dominant coupling mode, either intra or CFC and their strength. Our analysis focused on creating for the very first time a high accurate chronnectomic mapping of EEG brain connectivity into a valence-arousal 2D map. At first place, we focused on predicting participants' ratings of videos following a two-stage regression analysis for valence and arousal dimensions.

The rest of the paper is organized as follows: Section 2 describes the materials and section 3 describes the novelty of our advanced analytic pipeline. Section 4 is devoted to the results of the present study and, finally, section 5 discusses our findings in relationship with current literature.

II. MATERIALS

We studied the publicly available dataset, "DEAP: A Dataset for Emotion motion Analysis using Physiological Signals" [11]. It is a multimodal dataset for the analysis of human affective states.

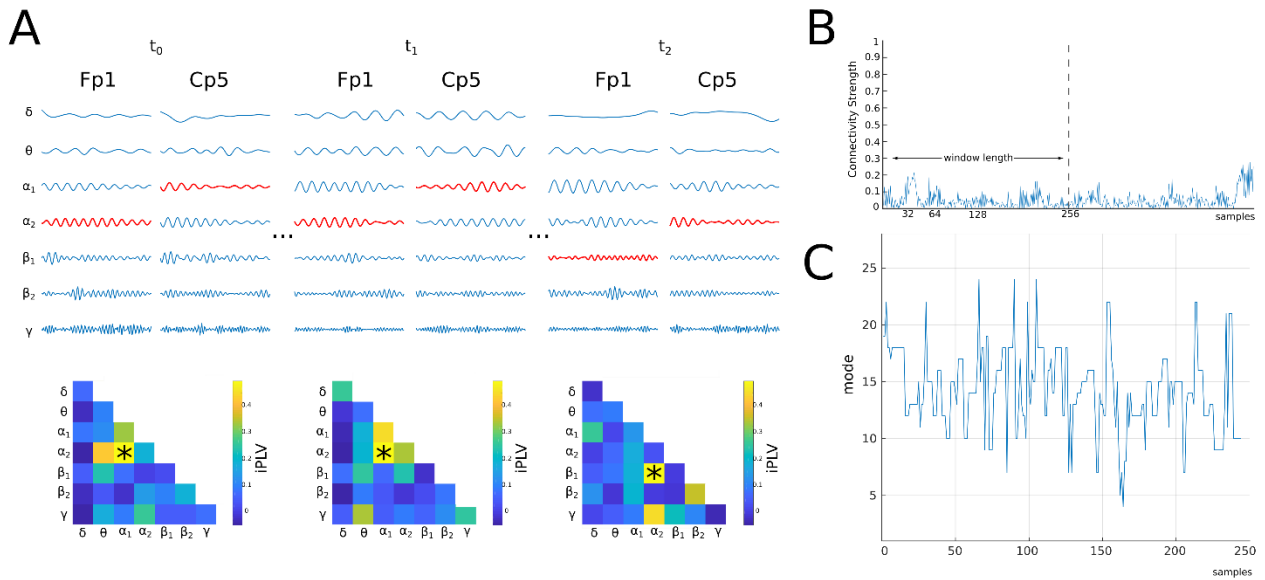


FIGURE 1. From Prominent Coupling Modes into Dominant Coupling Modes. An example from subject 1, first trial and for EEG pairs of Fp1 – Cp5. **A**) We demonstrated in three consecutive temporal segments the phase oscillations of the seven frequency bands for every EEG sensor. We denoted with red the dominant coupling mode between specific brain frequencies from the two EEG sensors. Below, every pair of plots of the phase time series, we tabulated in the so-called comodulograms the within and between frequency coupling index estimated via iPLV estimator. The dominant coupling mode in every temporal segment is denoted with '*' where in the first two temporal segments, the dominant coupling mode is stable $\alpha_1 - \alpha_2$ while in the third temporal segment it transits into $\alpha_2 - \beta_1$. **B**) The fluctuation of the functional coupling between Fp1 – Cp5 is illustrated as a time series. From this time series, we estimated detrended fluctuation analysis (^{TM}DFA). **C**) The transition behavior of dominant coupling mode across experimental time for Fp1 – Cp5 is demonstrated while the below comodulogram tabulates the probability distribution of the dominant coupling mode.

Thirty-two (32) Healthy participants (50% female), aged between 19 and 37 (mean age 26.9), were recruited to participate in the experiment.

The electroencephalogram (EEG) and an array of eight other peripheral physiological signals (including galvanic skin response, skin temperature, blood volume pressure, respiration rate, electromyogram and electrooculogram (horizontal and vertical) facial videos) were recorded while each one of subjects watched forty (40) one-minute long excerpts of music videos (Figure 1A). For some of the subjects, the facial videos were also obtained. The EEG setup included 32 active electrodes (channels) according to the international 10-20 system.

Afterwards, the subjects were assigned with the task of rating each video in terms of the levels of arousal, valence, like/dislike, and dominance by moving a computer mouse strictly horizontally over a scale of numbers from 1 to 9. A set of self-assessing manikins was displayed in the middle of the screen to help visualize these scales. For valence, this scale ranges from unhappy or sad to happy or joyful. For arousal, it ranges from calm or bored to stimulated or excited. For dominance, it ranges from submissive (or “without control”) to dominant (or “in control, empowered”). The liking index measures the participants’ tastes, not their feelings. For a comprehensive discussion about the experiment setup and protocol, the selection of the music videos, etc., the interested readers are encouraged to review the original paper [11].

Besides all the raw data and the original metadata (such as scores and demographics), the authors are kind enough to further provide a preprocessed alternative to the dataset, with downsampling to 128Hz applied and reordering of the electrodes already in place. We gained access to these data by following the given instructions; print, sign, and scan the provided EULA (End User License Agreement) and then return it via e-mail.

III. METHODS

The dynamic functional connectivity was estimated using a window sliding over a subject’s EEG recording. It was examined for the following seven brain frequencies ($\delta, \theta, \alpha_1, \alpha_2, \beta_1, \beta_2, \gamma$), defined respectively within the ranges (0.5-4 Hz; 4-8 Hz; 8-10 Hz; 10-13 Hz; 13-20 Hz; 20-30 Hz; 30.-45 Hz). We adopted a 3rd order Butterworth filters applied in a zero-phase mode to extract these characteristic brain rhythms using `filtfilt` MATLAB function.

A. CONSTRUCTION OF AN INTEGRATED DYNAMIC FUNCTIONAL CONNECTIVITY GRAPH (IDFCG)

To capture the multiplexity of human brain dynamics induced from music video clips, we adopted our DoCM model presented in our previous studies [30]–[34]. We first adopt a sliding window of 1sec moving its center by 5 ms towards the experimental time. As a proper functional connectivity estimator, we employed the imaginary part of phase clocking value (iPLV; 30-32) to estimate both within and between

frequencies functional interactions (Figure 1). During this process, we constructed seven within frequencies DFCG per trial and subject of size [trials x temporal segments x sensors x sensors]. To capture these cross-frequency couplings, we employed a very well-known and established method, namely phase-to-amplitude coupling (PAC) [35]. It quantifies the modulation between the oscillations of a lower frequency's phase and a higher frequency's amplitude. These interactions can be estimated within and between the sensors [36]–[41] based on the contents of the power-power, amplitude-amplitude, and amplitude-phase.

The steps to estimate PAC has been described in detail elsewhere [32], [39]. Shortly, we filtered the activity from one EEG sensor to a low-frequency (i.e. θ), and we extracted its instantaneous Hilbert phase. The EEG brain activity from the second sensor is filtered in a high-frequency (e.g. lower $\beta 1$) and computed its instantaneous Hilbert envelope. Subsequently, we filtered the instantaneous Hilbert envelope of the high-frequency signal within the range of the low-frequency range (θ component within the lower $\beta 1$), and we extracted its Hilbert phase dynamics. Finally, we adopted iPLV as a connectivity estimator to quantify the phase-locking that will reflect the PAC-interaction between the two involved brain rhythms. This phase-locking represents the degree to which the lower β ($\beta 1$) amplitude is comodulated with the θ phase. The outcome of this procedure is the construction of 21 DFCG between pairs of frequencies DFCG per trial and subject of size [trials x temporal segments x sensors x sensors]. This will give a total of 28 DFCG per trial and subject (Figure 1C).

The original phase-locking value is computed as:

$$PLV = \frac{1}{T} \sum_{t=1}^T e^{i(\varphi_k(t) - \varphi_l(t))} \quad (1)$$

and the iPLV is computed using the following:

$$iPLV = \frac{1}{T} |\Im \left(\sum_{t=1}^T e^{i(\varphi_k(t) - \varphi_l(t))} \right)| \quad (2)$$

In both cases, T denotes the number of samples under consideration and $\varphi(t)$ the instantaneous phase of the signal, as computed from Hilbert Transformation.

To detect the DoCM per pair of EEG sensors and temporal segments, we must adopt a proper surrogate analysis. In our previous studies [30]–[32], [39], we created 1.000 surrogate signals per EEG sensor, temporal segment, and for each of the seven frequency bands. Then, we estimated the 1.000 4D graphs (for each frequency band) to create a baseline distribution for each pair of EEG sensors, temporal segment, and potential coupling mode (28). Then, a p-value was assigned to each EEG sensor pair, temporal segment and coupling mode. Practically for every EEG pair at every temporal segment, we will get 28 p-values. By applying a Bonferroni-adjusted statistical threshold of $p < 0.01/28 = 0.000357$ to control for family-wise Type I error, we can get the DoCM. However, three cases must be taken into account: 1) only one DoCM survived the statistical threshold, 2) more than survived the

statistical threshold, and we decided to keep the one with the maximum iPLV value and 3) none of the potential coupling modes survived. In the end, we constructed personalized in a trial basis two IDFCG, one that kept the DoCM using numbers from 1 up to 28 {1 for δ , 2 for θ , ..., 7 for γ , 8 for $\delta - \theta$, ..., 28 for $\beta 2 - \gamma$ } (Figure 1C), and a second one that kept the iPLV value (Figure 1A).

B. DESCRIPTORS DERIVED FROM IDFCG

The application of our DoCM in a dynamic perspective provides us with an enriched description of the brain's connectivity within and between all frequencies' contents (cross-frequency coupling). This mapping captures the different underlying, unknown processes.

The outcome of our DoCM model can be tabulated in two 4D matrices M , of size *coupling modes* \times *temporal segments* \times *sensors* \times *sensors*. The first one stores the strength of the DoCM model, and the second the type of dominant coupling mode encoded with integers from 1 up to 28.

1) FLEXIBILITY INDEX

The Flexibility Index (FI) has been defined as the rhythm of change of dominant coupling mode between a pair of brain areas (here EEG pair of sensors) across experimental time [32], [33]. FI was estimated based on the second 4D matrix that keeps the dominant coupling mode. The following formula estimates it:

$$FI = \frac{\text{number of transitions}}{\text{number of temporal segments} - 1} \quad (3)$$

Which results in a matrix FI_{trial} is of size [*sensors* \times *sensors*] (Figure 2A). Based on our previous positive experience [30], [31], we selected FI as the leading component of our analysis. It is depicted in Figure 2C. The outcome of this analysis is a matrix of size [*sensors* \times *sensors*] per trial FI_{trial} .

2) DETRENDED FLUCTUATION ANALYSIS (DFA)

To analyze the fluctuation of the temporal coupling strength, we adopted DFA. DFA is a robust descriptor unsusceptible to non-stationary processes. Specifically in our study, the temporal autocorrelation structure of encephalographic activity and the functional coupling strength. Additionally, DFA, has been proven to be useful in untangling the long-range correlations in time series. DFA was estimated based on the first 4D matrix that stores iPLV coupling strength of the dominant coupling mode.

In a nutshell, to estimate the autocorrelation property of a signal $Y(t)$, the time series is divided into non-overlapping segments $Y_i(t)$, with $t = 1, \dots, n$ being discrete time steps and $i = 1, \dots, M$ indexing the temporal segments. $M = N/n$ denotes the number of non-overlapping segments of length n . In each segment the linear trend $y_i^{trend}(t)$ is removed (detrended) providing an estimate of fluctuations in terms of:

$$F_i(n) = \sqrt{\frac{1}{N} \sum_{t=1}^N (Y_i(t) - Y_i^{trend}(t))^2} \quad (4)$$

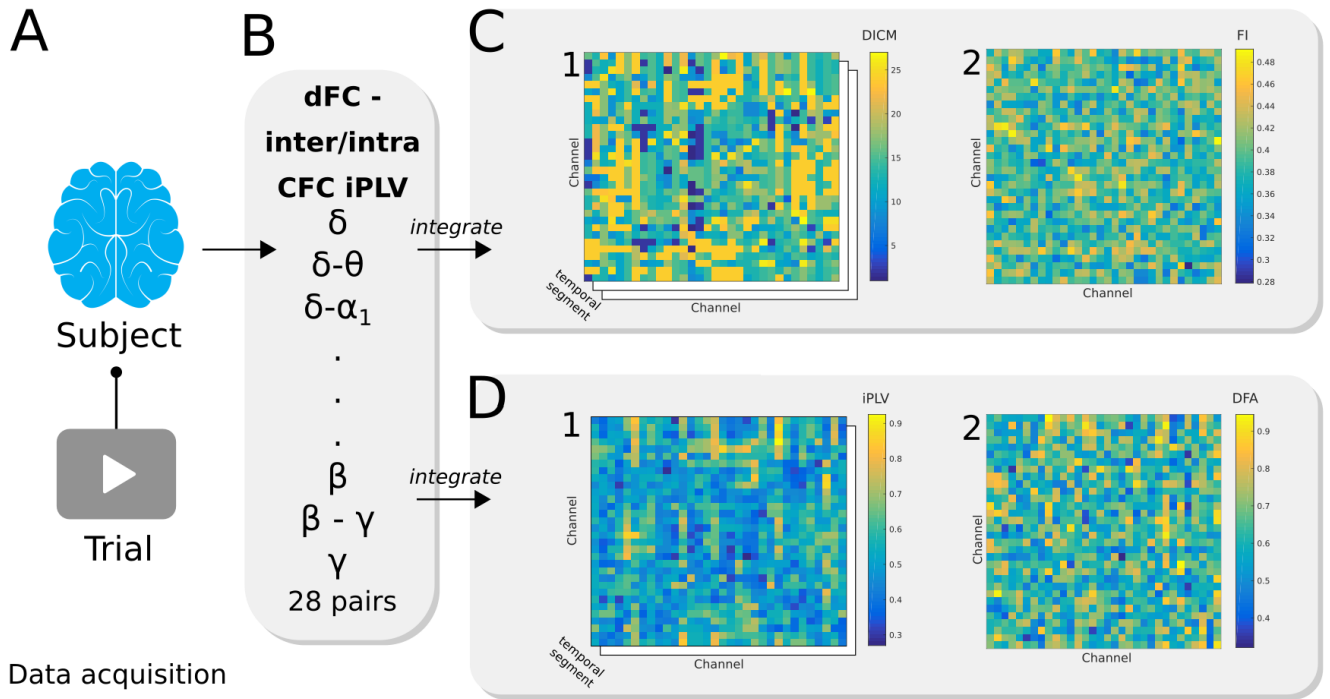


FIGURE 2. The data acquisition and feature extraction methodology applied to each subject and each music video. **A)** The electroencephalogram (EEG) of a subject is recorded while it watches a short excerpt, one minute, of a music video. **B)** We estimated dynamic functional connectivity graphs (DFCG) for each of within frequency bands (7 in total) and also for cross-frequency coupling modes between every pair of the basic frequency bands (21 in total), resulting into twenty-eight (28) potential coupling modes. This analysis was followed for every trial and independently for each subject **C.1)** Following a proper surrogate analysis, we revealed the dominant coupling mode (DoCM) for every pair of EEG sensors and for every temporal segment. The type of DoCM is stored in a 4D graph of size [trials \times temporal segments \times sensors \times sensors] **C.2)** The Flexibility Index (FI) is then computed from all temporal segments by polling each EEG sensor about its DoCM index's transitions between consecutive temporal segments. **D.1)** Similar to step (C) but we keep track of the connectivity iPLV value per pair of EEG sensors and temporal segments stored in a second 4D graph of size [trials \times temporal segments \times sensors \times sensors] and in **D.2)** we compute the Variance (VAR) of the fluctuations of functional connectivity strength across temporal segments per pair of EEG sensors as a simple index of the non-stationarity of dynamic functional connectivity.

This definition captures a set of fluctuations F_i that, in the presence of a power law are described with the equation $F_i(n, \tau) = n^\alpha \cdot F_i(\tau)$, which is equivalent to $\log(F_i) = \alpha \cdot \log(n) + \text{const}$. A linear relationship on a log-log plot indicates the presence of power law (fractal) scaling. The fluctuations can be characterized by a scaling exponent α , the slope of the line relating $\log F(n)$ to $\log n$. For further details regarding the estimation of DFA see the related article [40].

DFA has been estimated over the 1D time series that describe fluctuations of connectivity coupling across temporal segments for every pair of EEG sensors (Figure 1C). This feature constructs a matrix DFA_{trial} of size $sensors \times sensors$ (Figure 2D). We have previously used this estimator for dynamic functional connectivity analysis [41].

C. GRAPH CLUSTERING APPROACH FOR FEATURE SELECTION

In this section, we will describe the methodological approach we followed to construct the proposed graph-based feature selection.

We established a feature engineering process, that automatically extracts the most comprehensive features for each subject. First, we estimated the Pearson's correlation coefficients between all pair of sensors FIs across trials (Figure 3A),

resulting in a high-order, distance-like matrix M_{HO} of size 1024×1024 (Figure 3B).

Next, due to the size and nature of this distance matrix, we employed a topological filtering method based on Minimum Spanning Tree (MST) [43], called Orthogonal Minimum Spanning Tree (OMST) [33], [42]. MST has its roots in graph theory and has found its way to Neuroimaging with great impact [29]. It is an unbiased, assumption-free method that identifies significant links within a weighted graph, diminishing the need for statistical methods. OMST is an iterative, optimization procedure that computes an MST and estimates the Global Cost Efficiency. The objective function is given by:

$$J_{GCE}^{OMSTs} = GE - cost \tag{5}$$

where GE denotes the Global Efficiency of the network, a measure (as its name imply) of efficient information exchange. The $cost$, is the ratio of the sum of a MST's weights over the total sum of the initial, fully weighted graph.

This new, filtered graph is prone to contain another latent structure, in the form of a network community (Figure 3B). We probe this aspect with Newman's spectral community detection [44]. In short, it creates subdivisions of a network

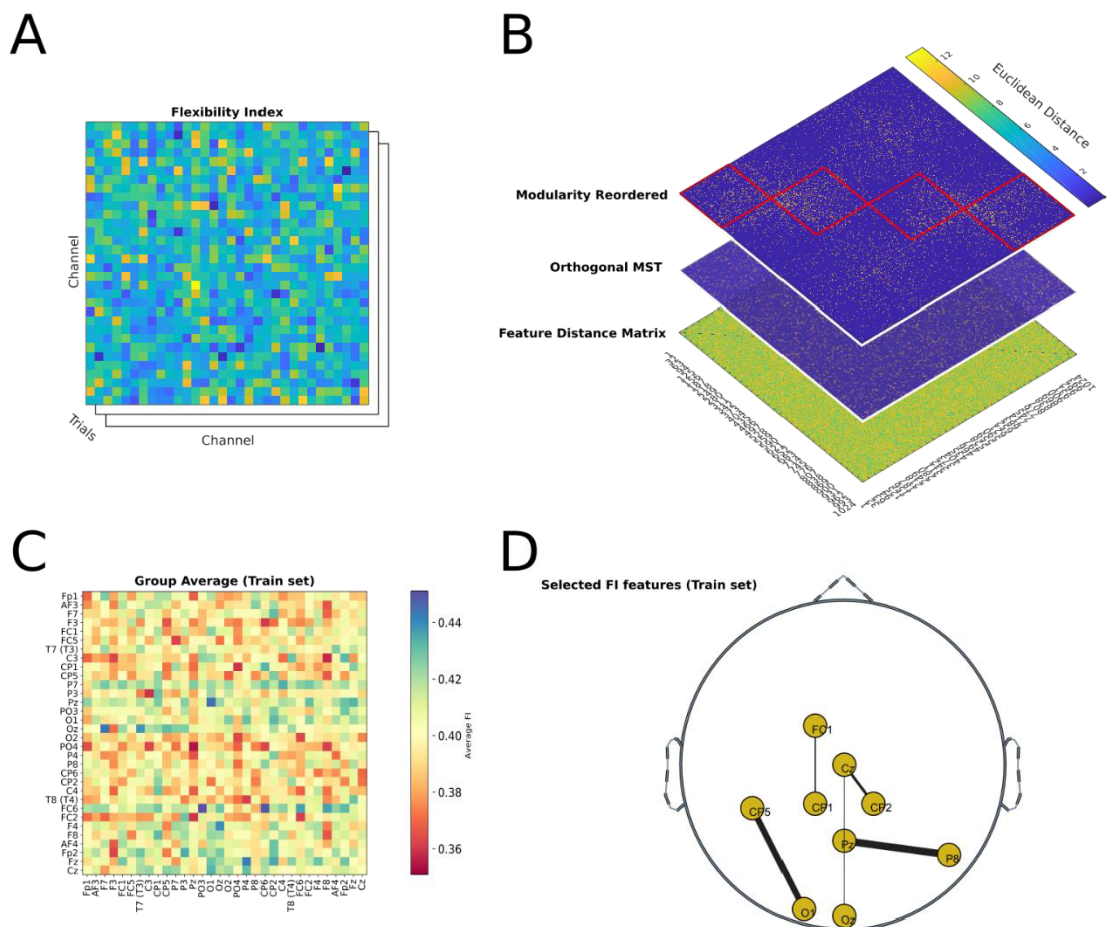


FIGURE 3. Model construction outline. **A)** The Flexibility Index is computed for each trial (music video). **B)** The lower layer depicts a distance matrix estimated from all the FIs, resulting into a high order graph. Subsequently, we use Orthogonal Minimum Spanning Trees and modularity to cluster the FIs. From each grouping, the FIs with the maximum distance correlation with Arousal or Valence are selected. **C)** The group average FI. **D)** The resulting FI topology of the robust selected FI-based connections across the 10 folds tailored to valence dimension. Thickness of the line connected a pair of EEG sensors decodes the number of times a feature is selected across the 10 - fold cross validation. Our results showed a high stability across the 10 folds ranging between 8 and an absolute 10 times selection.

into several groups so as the edges within a group are maximized while the ones between the groups are minimized [45]; it can be employed as a clustering method for graphs (Figure 3B).

Here, we detected associations between participant’s valence and arousal scores with either FIs or DFAs. We adopted Distance Correlation, denoted by R , which holds an important property that $R(x,y) = 0$ if and only if x and y are independent [46]. R index satisfies $0 \leq R \leq 1$, and it can estimate linear and non-linear relationships between two vectors in contrary to trivial Pearson’s correlation coefficient which can detect only linear associations.

Finally, from each grouping of pairs of edges, the FIs or DFAs with the maximum distance correlation [46] with arousal or valence are discovered. The accumulation of the selected FIs across all subjects and trials produce a comprehensive cohort map; as shown in Figure 3C and are back-projected as a topology in Figure 3D. Some features are more pronounced than others, hinting the possible existence of a

common underlying process. This mapping will be used to decide which features to include in the regression.

D. EXTREME LEARNING MACHINES

In the current study, the prediction of subjective participant’s valence and arousal score was realized as a regression problem. This model will map connectomic features derived from dynamic functional connectivity analysis (FI and DFA) to the subjective valence arousal evaluation. Here, we adopted extreme learning machines with kernels (RBF specifically in this study), as a highly efficient choice to handle difficult tasks without needing an extensive and demanding training session [47].

The ELM is an artificial feedforward neural network (ANN) with a single layer of hidden nodes. Weights of links connecting inputs to hidden nodes are randomly assigned while they never updated [48]. We adopted an RBF kernel for the regression analysis with ELM.

E. PREDICTION WITH REGRESSION

To construct an unbiased model, we separated the features, namely the Flexibility Index and the DFA, into a train and test set. Here, we built a ten-fold cross-validation on the integrated number of trials from the whole cohort. The total number of trials is equal to subjects \times trials = 32 \times 40 = 1280 trials.

Eventually, we followed the feature selection scheme described in section 3.3 for every training fold independently for valence/arousal and FIs/DFAs. From the extracted FI/DFA features, we built an ELM RBF regression model, for both the Arousal and Valence parameters. Finally, we computed the correlation (as well as their p -values) and the mean square error between the true values and the predicted ones.

F. STATIC NETWORKS AND FRONTAL ASYMMETRY INDEX

To compare the proposed scheme simultaneously with static brain networks, frontal asymmetry and within frequency interactions, we estimated the one frequency-dependent static FCG per frequency. Then, a laterality index (LI) was estimated by summing the functional strength between every possible pair of EEG sensors located over either left hemisphere (Fp1,F7,F3) or right hemisphere (Fp2,F8,F4) to investigate the hemispheric dominance associated with either frontal asymmetry of emotions:

$$LI = \frac{L - R}{L + R} \tag{6}$$

where L and R represent the total functional strength between the three frontal EEG sensors located over left or right hemisphere. LI values ranged between -1 and 1 .

A positive value of LI indicates left-hemisphere dominance, whereas a negative value OF LI indicates right-hemisphere dominance. This approach leads to a total of 8 LI per trial per subject. We followed the same validation approach as for FI and DFA, which is described in sections D and E.

G. THE MULTIPLEX CONNECTOMIC BIOMARKER OF VALENCE-AROUSAL MAP

The connectomic biomarkers related to valence and arousal have been extracted based on the spatiotemporal evolution of both the type (FI) and the strength (DFA) of dominant coupling modes. We aimed to define a robust and universal connectomic biomarker for both dimensions of the valence-arousal map. Towards this strategy, we extracted two basic features to quantify the fluctuations of dominant coupling mode and its functional strength between every pair of EEG sensors across experimental time. To the best of our knowledge, this is the very first study in emotional BCI systems that adopted a dynamic integrated (multiplex) dynamic functional connectivity analysis. Here, the adopted scheme integrates both within and between frequencies couplings in a single-layer integrated dynamic functional connectivity graph under DoCM model [30], [31].

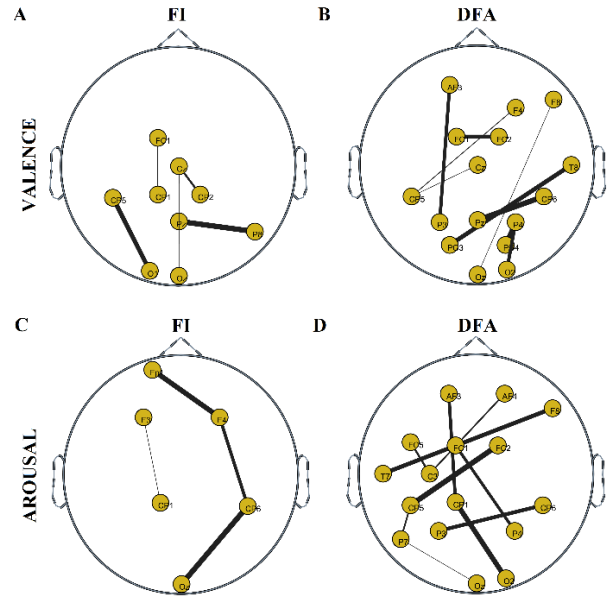


FIGURE 4. Topological layouts of the robust FI and DFA based connections that contributed the most to the overall prediction of valence and arousal emotional dimension. FI based connections for the best prediction of A) valence and C) arousal dimension. DFA based connections for the best prediction of B) valence and D) arousal dimension.

Figure 4 illustrates the topology of selected FI and DFA based connections as features that best predict both valence and arousal dimensions. FI-based connections are located over fronto-central, parietal, and occipital brain areas for valence (Figure 4A) and frontal, centroparietal, and occipital for arousal (Figure 4C). DFA-based connections are located over frontal, fronto-central, centro-parietal parietal, temporal, and occipital brain areas in both valence and arousal dimensions. A few connections are distributed between brain areas located over both hemispheres (bilateral) (Figure 4 B, D).

H. DISTANCE CORRELATION BETWEEN SELECTED FEATURES AND SUBJECTIVE AFFECTIVE RATINGS

Figure 5 demonstrates the distance correlation between subjects' ratings and the ones predicted by the proposed pipeline. The FI outperformed DFA; meaning that the transition of dominant coupling mode is more informative than the fluctuations of functional strength. Figure 6 depicts the distance correlation of FI and DFA. Figure 4 shows the FA and DFA topological features with the subjects' subjective rating of valence and arousal. Figure 7 illustrates quantitatively and schematically the performance of FI and DFA to the prediction of 2D affective space. FI outperformed DFA across the whole 2D affective space.

I. EVALUATION OF THE PROPOSED SCHEME

The average mean squared error across 10 folds was: a) for FI, 0.56 and 0.58 for valence and arousal, correspondingly and b) for DFA, 1.92 and 1.96 for valence and arousal, accordingly and c) for LI, 1.65 and 1.78 for valence and arousal, accordingly. To enhance the visualization of the proposed

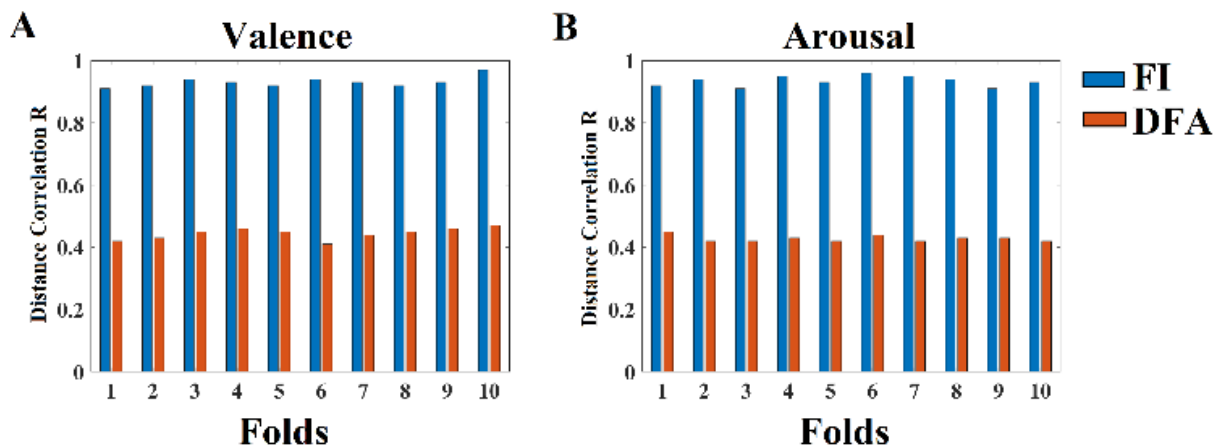


FIGURE 5. Histograms depicting the correlation scores between the true values and the values predicted from our model per fold, when trained with the FI and DFA features for both the A) Arousal and B) Valence.

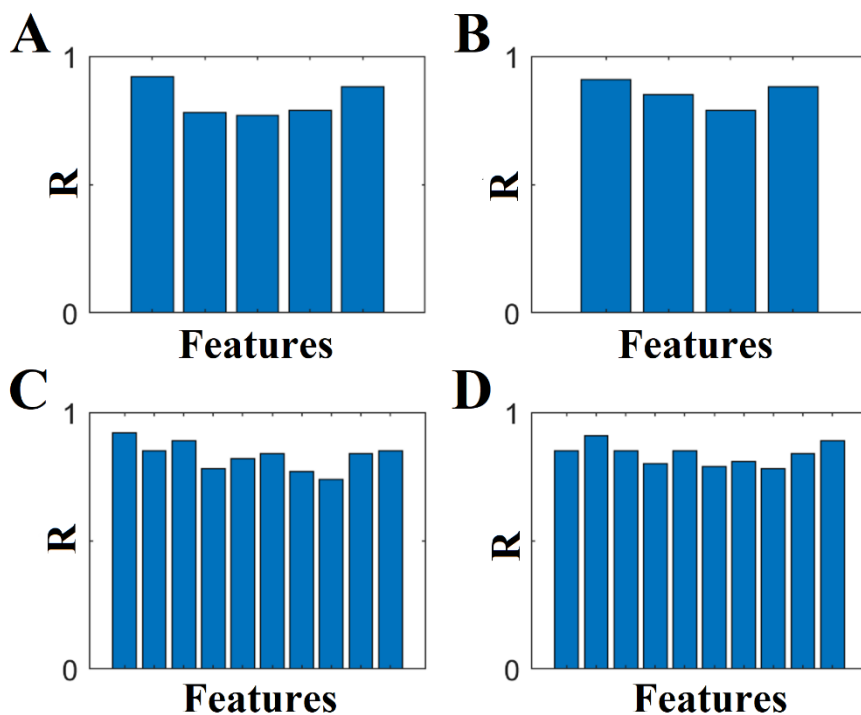


FIGURE 6. Distance correlation between the FI and DFA selected features shown in Figure 5 with the subjective ratings of valence and arousal from the participants. A) FI - Valence, B) FI - Arousal, C) DFA - Valence and D) DFA - Arousal (R - Distance Correlation).

predicted scheme under DICM model, we illustrated every trial in the 2D affective map as a circle with its radius to be analogous to the sum of MSE in both dimensions (Figure 7). FI outperformed DFA in both emotional dimensions.

IV. DISCUSSION

Our paper reports in detail out attempts to create an accurate multiplex connectomic mapping of 2D affective model under the framework of dynamic functional connectivity analysis and EEG recordings. It is also a proof of concept for the potential feasibility of emotional BCI systems that support

an interface between a subject for a specific application or disease groups (e.g. depressive, schizophrenic etc.) and a personal computer.

Our results support the efficacy of the multiplexity integrated framework presented here. Regarding, the small number of EEG sensors, it further attributes the our framework that it can be computed fast enough to support neurofeedback BCI systems [40], [50]. The main advantage of the current approach is that it can be evaluated in EEG wearable devices like emotive, Muse EEG portable devices supporting a low cost personalized in house treatment.

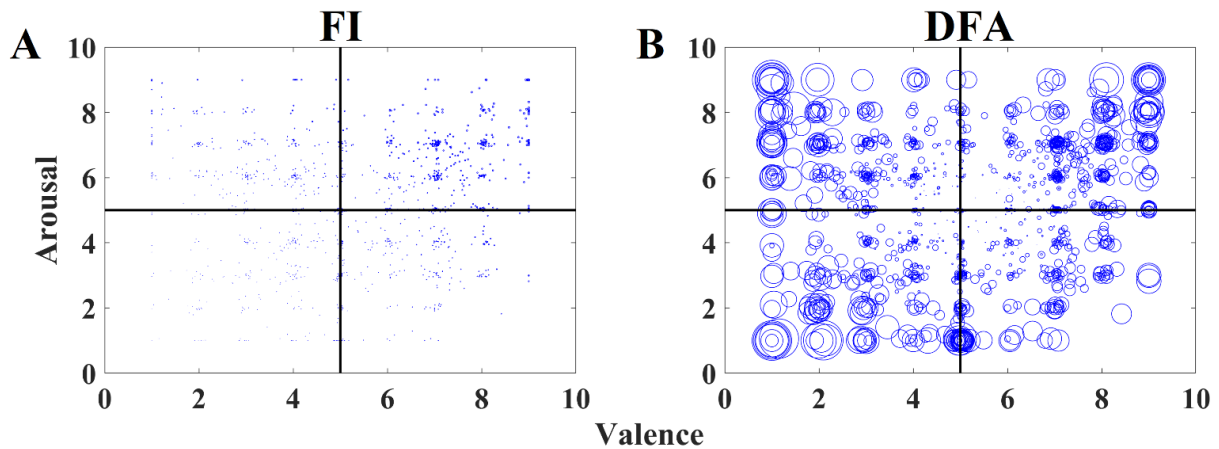


FIGURE 7. Illustrating the predicted valence and arousal values as 2D circles with their dimension corresponding to the mean square error between subjective ratings and predicted via FI and DFA. A) Predicted affective score with FI and B) Predicted affective score with DFA.

This study is the first one that attempted to approach the difficult problem of identifying EEG connectomic biomarkers under a dynamic functional connectivity framework. Additionally, we adopted our DoCM model that integrates into a single dynamic functional connectivity graph the dominant coupling modes from both within and between frequency coupling modes [30], [31]. Estimating the transition rate of dominant coupling modes across experimental time via FI proved a more efficient chronnectomic biomarker compared to the long-range autocorrelation behaviour of the fluctuations of coupling strength estimated via DFA descriptor (Figure 7). The LI, as estimated over static frequency-dependent FCGs, performed poorly. Frontal asymmetries were not evaluated in our project. Our whole-brain, dynamic and integrated approach proved valuable for valence and arousal recognition.

However, in the present study, we analyzed EEG recordings without addressing the contribution of potential artifacts. Before the application of such a system in a real scenario, the issue of artifact suppression should be addressed, for example, using independent component analysis [51] or empirical mode decomposition [52].

Nowadays, we live in the era of digital technologies that are part of our daily activities from preventive medicine to interconnectedness of devices in our homes. However, the missing piece of this highly complex technology is people. To enable scenarios like the one proposed here to move from a lab-oriented environment to a daily clinical or not applicable, we must present realistic BCI scenarios that can ideally adjust subjectively to every target scenario and group [53].

V. CONCLUSION

In this study, we have presented a framework of studying emotions elicited while subjects were viewing music videos via electroencephalographic recordings. Our analysis focused on dynamic functional connectivity approach with the incorporation of both within frequencies and between

frequencies coupling modes the so-called cross-frequency coupling. Adopting our recent dominant coupling mode (DoCM) model, we untangled the preferred coupling mode per pair of EEG sensors and across experimental time. Then, a flexibility index was defined to capture the fluctuation of the dominant coupling mode between consecutive temporal segments. Fluctuations of temporal coupling strength of dominant coupling modes have been studied via detrended fluctuation analysis. Our research focused on identifying the best set of EEG pairs of sensors across the cohort that can predict valence and arousal personalized ratings with high accuracy. Flexibility index proved a more informative descriptor of nested oscillations compared to its counterpart the detrended fluctuation analysis.

We live in the digital age of designing human-centered products and services from consumer electronics, medical devices to medical and entertainment applications. Exploring affective responses elicited by music and studying through electroencephalography can support personalized music recommendation systems via an adaptive loop between music libraries (e.g. Spotify) and dynamic consumer rating. Our framework could benefit researchers that explore how emotions are elicited from positive-negative emotional images in depression, in Alzheimer's disease and other target brain disorders in multiple ways. In the future, we would like to test the whole analysis in a similar study recorded with a low-cost device like the emotive EEG headset.

REFERENCES

- [1] T. Baumgartner, M. Esslen, and L. Jäncke, "From emotion perception to emotion experience: Emotions evoked by pictures and classical music," *Int. J. Psychophysiol.*, vol. 60, no. 1, pp. 34–43, Apr. 2006.
- [2] S. R. Fussell, "The verbal communication of emotion: Introduction and overview," in *The Verbal Communication of Emotions*. London, U.K.: Psychology Press, 2002, pp. 9–24.
- [3] J. L. Tracy, D. Randles, and C. M. Steckler, "The nonverbal communication of emotions," *Current opinion Behav. Sci.*, vol. 3, pp. 25–30, Jun. 2015.

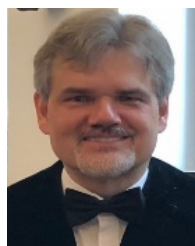
- [4] S. Makeig, G. Leslie, T. Mullen, D. Sarma, N. Bigdely-Shamlo, and C. Kothe, "First demonstration of a musical emotion BCI," in *Proc. Int. Conf. Affect. Comput. Intell. Interact.*, 2011, pp. 487–496.
- [5] S. Taran and V. Bajaj, "Emotion recognition from single-channel EEG signals using a two-stage correlation and instantaneous frequency-based filtering method," *Comput. Methods Programs Biomed.*, vol. 173, pp. 157–165, May 2019.
- [6] R. W. Picard, E. Vyzas, and J. Healey, "Toward machine emotional intelligence: Analysis of affective physiological state," *IEEE Trans. Pattern Anal. Mach. Intell.*, vol. 23, no. 10, pp. 1175–1191, Oct. 2001.
- [7] R. Ramirez, M. Palencia-Lefler, S. Giraldo, and Z. Vamvakousis, "Musical neurofeedback for treating depression in elderly people," *Frontiers Neurosci.*, vol. 9, p. 354, Oct. 2015.
- [8] P. N. Juslin and J. A. Sloboda, "Music and emotion," *Psychol. Music*, vol. 3, pp. 583–645, 2013.
- [9] D. A. Adamos, S. I. Dimitriadis, and N. A. Laskaris, "Towards the bio-personalization of music recommendation systems: A single-sensor EEG biomarker of subjective music preference," *Inf. Sci.*, vols. 343–344, pp. 94–108, May 2016.
- [10] R. Ramirez and Z. Vamvakousis, "Detecting emotion from EEG signals using the emotive epic device," in *Proc. Int. Conf. Brain Inform.* Berlin, Germany: Springer, Dec. 2012, pp. 175–184.
- [11] S. Koelstra, C. Muhl, M. Soleymani, J.-S. Lee, A. Yazdani, T. Ebrahimi, T. Pun, A. Nijholt, and I. Patras, "DEAP: A database for emotion analysis; Using physiological signals," *IEEE Trans. Affect. Comput.*, vol. 3, no. 1, pp. 18–31, Jan. 2012.
- [12] J. Liu, H. Meng, M. Li, F. Zhang, R. Qin, and A. K. Nandi, "Emotion detection from EEG recordings based on supervised and unsupervised dimension reduction," *Concurrency Comput., Pract. Exper.*, vol. 30, no. 23, p. e4446, Dec. 2018.
- [13] M. Chen, J. Han, L. Guo, J. Wang, and I. Patras, "Identifying valence and arousal levels via connectivity between EEG channels," in *Proc. Int. Conf. Affect. Comput. Intell. Interact. (ACII)*, Sep. 2015, pp. 63–69.
- [14] W.-L. Zheng, J.-Y. Zhu, and B.-L. Lu, "Identifying stable patterns over time for emotion recognition from EEG," *IEEE Trans. Affect. Comput.*, vol. 10, no. 3, pp. 417–429, Jul./Sep. 2019.
- [15] X. Chen, H. Zhang, L. Zhang, C. Shen, S. Lee, and D. Shen, "Extraction of dynamic functional connectivity from brain grey matter and white matter for MCI classification," *Hum. Brain Mapping*, vol. 38, no. 10, pp. 5019–5034, Oct. 2017.
- [16] P. Li, H. Liu, Y. Si, C. Li, F. Li, X. Zhu, X. Huang, Y. Zeng, D. Yao, Y. Zhang, and P. Xu, "EEG based emotion recognition by combining functional connectivity network and local activations," *IEEE Trans. Biomed. Eng.*, vol. 66, no. 10, pp. 2869–2881, Oct. 2019.
- [17] X. Liu, T. Li, C. Tang, T. Xu, P. Chen, A. Bezerianos, and H. Wang, "Emotion recognition and dynamic functional connectivity analysis based on EEG," *IEEE Access*, vol. 7, p. 143 293-143 302, 2019.
- [18] J. Li, H. Ji, R. Gu, L. Hou, Z. Zhang, Q. Wu, R. Lu, and M. Li, "Explore the brain response to naturalistic and continuous music using EEG phase characteristics," in *Proc. Int. Conf. Intell. Comput. (ICIC)*, 2016, pp. 294–305.
- [19] X. Ding and S.-W. Lee, "Changes of functional and effective connectivity in smoking replenishment on deprived heavy smokers: A resting-state fMRI study," *PLoS ONE*, vol. 8, no. 3, Mar. 2013, Art. no. e59331.
- [20] Y. Dasdemir, E. Yildirim, and S. Yildirim, "Analysis of functional brain connections for positive–negative emotions using phase locking value," *Cognit. Neurodyn.*, vol. 11, no. 6, pp. 487–500, Dec. 2017.
- [21] P. Kurt, K. Eroğlu, T. Bayram Kuzgun, and B. Güntekin, "The modulation of delta responses in the interaction of brightness and emotion," *Int. J. Psychophysiol.*, vol. 112, pp. 1–8, Feb. 2017.
- [22] Y.-P. Lin, C.-H. Wang, T.-P. Jung, T.-L. Wu, S.-K. Jeng, J.-R. Duann, and J.-H. Chen, "EEG-based emotion recognition in music listening," *IEEE Trans. Biomed. Eng.*, vol. 57, no. 7, pp. 1798–1806, Jul. 2010.
- [23] Z. Mohammad Alipour, S. Mohammadkhani, and R. Khosrowabadi, "Alteration of perceived emotion and brain functional connectivity by changing the musical rhythmic pattern," *Exp. Brain Res.*, vol. 237, no. 10, pp. 2607–2619, Oct. 2019.
- [24] C. W. E. M. Quaedflieg, F. T. Y. Smulders, T. Meyer, F. Peeters, H. Merckelbach, and T. Smeets, "The validity of individual frontal alpha asymmetry EEG neurofeedback," *Social Cognit. Affect. Neurosci.*, vol. 11, no. 1, pp. 33–43, Jan. 2016.
- [25] Z. Wang, Y. Tong, and X. Heng, "Phase-locking value based graph convolutional neural networks for emotion recognition," *IEEE Access*, vol. 7, p. 93 711-93 722, 2019.
- [26] G. G. Berntson, G. J. Norman, and J. T. Cacioppo, "Comment: Laterality and evaluative bivalence: A neuroevolutionary perspective," *Emotion Rev.*, vol. 3, no. 3, pp. 344–346, Jul. 2011.
- [27] M. Palmiero and L. Piccardi, "Frontal EEG asymmetry of mood: A mini-review," *Frontiers Behav. Neurosci.*, vol. 11, p. 224, Nov. 2017.
- [28] D. T. Hettich, E. Bolinger, T. Matuz, N. Birbaumer, W. Rosenstiel, and M. Spüler, "EEG responses to auditory stimuli for automatic affect recognition," *Frontiers Neurosci.*, vol. 10, p. 244, Jun. 2016.
- [29] Y.-Y. Lee and S. Hsieh, "Classifying different emotional states by means of EEG-based functional connectivity patterns," *PLoS ONE*, vol. 9, no. 4, Apr. 2014, Art. no. e95415.
- [30] S. I. Dimitriadis, "Complexity of brain activity and connectivity in functional neuroimaging," *J. Neurosci. Res.*, vol. 96, no. 11, pp. 1741–1757, Nov. 2018.
- [31] S. I. Dimitriadis and C. I. Salis, "Mining time-resolved functional brain graphs to an EEG-based chronnectomic brain aged index (CBAI)," *Frontiers Hum. Neurosci.*, vol. 11, p. 423, Sep. 2017.
- [32] S. I. Dimitriadis, N. A. Laskaris, P. G. Simos, J. M. Fletcher, and A. C. Papanicolaou, "Greater repertoire and temporal variability of cross-frequency coupling (CFC) modes in resting-state neuromagnetic recordings among children with reading difficulties," *Frontiers Hum. Neurosci.*, vol. 10, p. 163, Apr. 2016.
- [33] S. I. Dimitriadis, M. Antonakakis, P. Simos, J. M. Fletcher, and A. C. Papanicolaou, "Data-driven topological filtering based on orthogonal minimal spanning trees: Application to multigroup magnetoencephalography resting-state connectivity," *Brain Connectivity*, vol. 7, no. 10, pp. 661–670, Dec. 2017.
- [34] S. I. Dimitriadis, P. G. Simos, J. M. Fletcher, and A. C. Papanicolaou, "Aberrant resting-state functional brain networks in dyslexia: Symbolic mutual information analysis of neuromagnetic signals," *Int. J. Psychophysiol.*, vol. 126, pp. 20–29, Apr. 2018.
- [35] B. Voytek, R. T. Canolty, A. Shestuyuk, N. Crone, J. Parvizi, and R. T. Knight, "Shifts in gamma phase–amplitude coupling frequency from theta to alpha over posterior cortex during visual tasks," *Frontiers Hum. Neurosci.*, vol. 4, p. 191, Oct. 2010.
- [36] G. Buzsáki, "Neural syntax: Cell assemblies, synapse ensembles, and readers," *Neuron*, vol. 68, no. 3, pp. 362–385, Nov. 2010.
- [37] R. T. Canolty and R. T. Knight, "The functional role of cross-frequency coupling," *Trends Cognit. Sci.*, vol. 14, no. 11, pp. 506–515, Nov. 2010.
- [38] G. Buzsáki, N. Logothetis, and W. Singer, "Scaling brain size, keeping timing: Evolutionary preservation of brain rhythms," *Neuron*, vol. 80, no. 3, pp. 751–764, Oct. 2013.
- [39] S. I. Dimitriadis, N. A. Laskaris, M. P. Bitzidou, I. Tarnanas, and M. N. Tsolaki, "A novel biomarker of amnesic MCI based on dynamic cross-frequency coupling patterns during cognitive brain responses," *Frontiers Neurosci.*, vol. 9, p. 350, Oct. 2015.
- [40] C.-K. Peng, S. Havlin, H. E. Stanley, and A. L. Goldberger, "Quantification of scaling exponents and crossover phenomena in nonstationary heartbeat time series," *Chaos, Interdiscipl. J. Nonlinear Sci.*, vol. 5, no. 1, pp. 82–87, Mar. 1995.
- [41] S. I. Dimitriadis, N. A. Laskaris, P. G. Simos, S. Micheloyannis, J. M. Fletcher, R. Rezaie, and A. C. Papanicolaou, "Altered temporal correlations in resting-state connectivity fluctuations in children with reading difficulties detected via MEG," *NeuroImage*, vol. 83, pp. 307–317, Dec. 2013.
- [42] S. I. Dimitriadis, C. Salis, I. Tarnanas, and D. E. Linden, "Topological filtering of dynamic functional brain networks unfolds informative chronnectomics: A novel data-driven thresholding scheme based on orthogonal minimal spanning trees (OMSTs)," *Frontiers Neuroinform.*, vol. 11, p. 28, Apr. 2017.
- [43] J. B. Kruskal, Jr., "On the shortest spanning subtree of a graph and the traveling salesman problem," *Proc. Amer. Math. Soc.*, vol. 7, no. 1, pp. 48–50, Feb. 1956.
- [44] M. E. J. Newman, "Modularity and community structure in networks," *Proc. Nat. Acad. Sci. USA*, vol. 103, no. 23, pp. 8577–8582, Jun. 2006.
- [45] M. Rubinov and O. Sporns, "Complex network measures of brain connectivity: Uses and interpretations," *NeuroImage*, vol. 52, no. 3, pp. 1059–1069, Sep. 2010.

- [46] G. J. Székely and M. L. Rizzo, "Partial distance correlation with methods for dissimilarities," *Ann. Statist.*, vol. 42, no. 6, pp. 2382–2412, Dec. 2014.
- [47] G.-B. Huang, Q.-Y. Zhu, and C.-K. Siew, "Extreme learning machine: Theory and applications," *Neurocomputing*, vol. 70, nos. 1–3, pp. 489–501, Dec. 2006.
- [48] G.-B. Huang, "What are extreme learning machines? Filling the gap between frank Rosenblatt's dream and John von Neumann's puzzle," *Cognit. Comput.*, vol. 7, no. 3, pp. 263–278, Jun. 2015.
- [49] V. Lorenzetti, B. Melo, R. Basilio, C. Suo, M. Yücel, C. J. Tierra-Criollo, and J. Moll, "Emotion regulation using virtual environments and real-time fMRI neurofeedback," *Frontiers Neurol.*, vol. 9, p. 390, Jul. 2018.
- [50] D. J. McFarland, J. Daly, C. Boulay, and M. A. Parvaz, "Therapeutic applications of BCI technologies," *Brain-Comput. Interface*, vol. 4, nos. 1–2, pp. 37–52, Apr. 2017.
- [51] M. T. Akhtar, T.-P. Jung, S. Makeig, and G. Cauwenberghs, "Recursive independent component analysis for online blind source separation," in *Proc. IEEE Int. Symp. Circuits Syst.*, May 2012, pp. 2813–2816.
- [52] N. E. Huang, Z. Shen, S. R. Long, M. C. Wu, H. H. Shih, Q. Zheng, N.-C. Yen, C. C. Tung, and H. H. Liu, "The empirical mode decomposition and the Hilbert spectrum for nonlinear and non-stationary time series analysis," *Proc. Roy. Soc. London A, Math., Phys. Eng. Sci.*, vol. 454, no. 1971, pp. 903–995, Mar. 1998.
- [53] H. J. Baek, M. H. Chang, J. Heo, and K. S. Park, "Enhancing the usability of brain-computer interface systems," *Comput. Intell. Neurosci.*, vol. 2019, pp. 1–12, Jun. 2019.



STAVROS I. DIMITRIADIS was born in Thessaloniki, Greece, in 1978. He received the bachelor's degree in computer science and the master's degree in digital media from the Department of Informatics, Aristotle University of Thessaloniki, Thessaloniki, in 2008 and 2010, respectively, and the Ph.D. degree in neuroinformatics from an Interdepartmental Master Programme of Physics, Biology, Computer Science, Medicine, and the Department of Electrical Engineering and Com-

puter Technology, University of Patras, Greece. His Ph.D. has been awarded from the National Research Centre as the Best Ph.D. in Greece for 2013. In 2013, he started working as a Postdoctoral Researcher in the Artificial Intelligence and Information Analysis Laboratory, Department of Informatics. He was also a member of the Neuroinformatics Group, Thessaloniki. In 2015, he joined the School of Medicine, Cardiff, U.K., as a Research Fellow working on the biggest NeuroImaging Centre in EU and the Cardiff University Brain Research Imaging Centre (CUBRIC), Cardiff. He has been trained in data acquisition with state-of-the-art neuroimaging modalities MEG/MRI/DTI/fMRI and in genetic analysis in collaboration with experts. He has been working under MRC Grant (Behavioral and Neurophysiological Effects of Schizophrenia Risk Genes: A Multi-Locus, Pathway Based Approach) in a Pioneer Project, where he collected with his colleagues a big unique cohort from 200 subjects with multimodal neuroimaging, including genetics. Since 2017, he has been working as a Research Fellow with the CUBRIC Neuroimaging Centre awarded a prestigious MARIE-CURIE COFUND EU-UK. He has already published more than 50 publications in journal (38 as first author) and more than 20 in international conferences with peer review. His research interests include neuroinformatics, network neuroscience, neuroimaging, computational intelligence, biomarkers for various brain disorders and diseases, aging, schizophrenia, Alzheimer's disease, mild traumatic brain injury, genetic neuroimaging, and bioinformatics. He also serves as an Editorial Member for *Clinical Neurophysiology* and *Frontiers in Neuroinformatics* journals. He has served as a Guest Editor in special issues in *PLOS One* and *Brain Sciences* journals.



RAINER GOEBEL studied psychology and computer science in Marburg, Germany, in 1983 and 1988, respectively. He received the Ph.D. degree from the Technical University Braunschweig, Germany, in 1994. He also received the Heinz Maier Leibnitz Advancement Award in cognitive science in 1993 sponsored by the German Minister of Science and Education for a publication on the binding problem, and the Heinz Billing Award from the Max Planck Society in 1994 for devel-

oping a software package for the creation and simulation of neural network models. From 1995 to 1999, he was a Postdoctoral Fellow with the Max Planck Institute for Brain Research in Frankfurt/Main, where he founded the Functional Neuroimaging Group. Since January 2000, he has been a Full Professor of cognitive neuroscience with Maastricht University, The Netherlands. He is currently the Founding Director of the Maastricht Brain Imaging Centre (M-BIC) and the driving force of the recently established ultra-high field imaging center housing 3, 7, and 9.4 Tesla human MRI scanners. From 2008 to 2017, he was a Team Leader of the Modeling and Neuroimaging group, Netherlands Institute for Neuroscience, Amsterdam. He has served as the Chair of the Organization for Human Brain Mapping from 2006 to 2008. In 2014, he became a member of the Royal Netherlands Academy of Arts and Sciences. In 2017, he became a member of the German National Academy of Science (Leopoldina). He received funding for basic and applied neuroscience research, including an ERC Advanced Investigators Grant from 2011 to 2016 and continued funding from the Human Brain Project (HBP) since 2013. He is also the Founder and the CEO of company Brain Innovation B.V., Maastricht, The Netherlands, developing software for neuroimaging data analysis.



AVRAAM D. MARIMPIS received the M.Sc. degree from the Department of Computer Science, Aristotle University of Thessaloniki. He is currently pursuing the Ph.D. degree with the Department of Cognitive Neuroscience, Faculty of Psychology and Neuroscience, Maastricht University, Maastricht, The Netherlands. He is also employed as a Software Engineer and a Research and Development Engineer at Brain Innovation B.V., Maastricht. His research interests include

brain connectivity, connectomics, chronnectomics, and graph theory.

...